

Distribution Agreement

In presenting this thesis as a partial fulfillment of the requirements for a degree from Emory University, I hereby grant to Emory University and its agents the non-exclusive license to archive, make accessible, and display my thesis in whole or in part in all forms of media, now or hereafter now, including display on the World Wide Web. I understand that I may select some access restrictions as part of the online submission of this thesis. I retain all ownership rights to the copyright of the thesis. I also retain the right to use in future works (such as articles or books) all or part of this thesis.

Rachel Seong

April 10, 2024

Investigation of ectopic changes between healthy and Ataxia Telangiectasia cells

by

Rachel Seong

Bing Yao
Adviser

Biology

Bing Yao
Adviser

Peng Jin
Committee Member

Leila Rieder
Committee Member

2024

Investigation of ectopic changes between healthy and Ataxia Telangiectasia cells

By

Rachel Seong

Bing Yao

Adviser

An abstract of
a thesis submitted to the Faculty of Emory College of Arts and Sciences
of Emory University in partial fulfillment
of the requirements of the degree of
Bachelor of Science with Honors

Biology

2024

Abstract

Investigation of ectopic changes between healthy and Ataxia Telangiectasia cells

By Rachel Seong

Ataxia Telangiectasia (AT) affects 1 in 40,000 to 100,000 people. It is an autosomal recessive neurodegenerative disease that affects the part of the brain that controls motor movement.

Mutations in the ataxia telangiectasia mutated (ATM) gene cause the disease, so we wanted to explore the differences in various parts of the DNA damage response pathway, such as γ H2A.X, 53BP1, R-loops, and ATM, between healthy cells and AT patient-derived cells, more specifically in neural progenitor cells from age-matched healthy controls and AT patients. To investigate the differences, ionizing radiation was done to induce DNA damage in both the control and AT cell lines and given different recovery time points, which was followed by immunofluorescence staining on γ H2A.X and 53BP1, as well as western blots to quantify the levels of γ H2A.X. We discovered that the increase in γ H2A.X levels was not as significant in AT cells when compared to the controls. Additionally, dot blots were used to assess global R-loop changes in AT cells, in which R-loop accumulation was higher in AT cells, with a further increase in R-loop accumulation after IR treatment. qPCR sequencing was done to compare ATM mRNA expression, and we discovered that there were lower levels of ATM mRNA expression in AT cells. From the data, we can conclude that AT is potentially caused by dysregulation of the DDR pathway, specifically through impairment or less transcription of ATM.

Investigation of ectopic changes between healthy and Ataxia Telangiectasia cells

By

Rachel Seong

Bing Yao

Adviser

A thesis submitted to the Faculty of Emory College of Arts and Sciences
of Emory University in partial fulfillment
of the requirements of the degree of
Bachelor of Science with Honors

Biology

2024

Acknowledgements

Yao Lab

Bing Yao, Ph.D.

Katherine Westover

Yingzi Hou, Ph.D.

Paula Martinez-Feduchi

Yangping Li, Ph.D.

Feng Wang, Ph.D.

Yilin Wang, MPH

Honors Committee

Peng Jin, Ph.D.

Leila Rieder, Ph.D.

Table of Contents

Abstract

Introduction

Methods and Materials

Cell-Line Information

Reprogramming LCLs and Fibroblasts

Ionizing Radiation (IR)

RT-qPCR

Immunofluorescence Staining

Western Blots

gDNA Isolation

Dot Blots

Results

AT Cells Present Lower Expression of ATM mRNA

Differences in γ H2A.X and 53BP1 Levels Between Healthy and AT Cells

R-loop Accumulation in AT

Discussion

AT Cells Present Lower Expression of ATM mRNA

Differences in γ H2A.X and 53BP1 Levels Between Healthy and AT Cells

R-loop Accumulation in AT

References

Abstract

Ataxia Telangiectasia (AT) affects 1 in 40,000 to 100,000 people. It is an autosomal recessive neurodegenerative disease that affects the part of the brain that controls motor movement.

Mutations in the ataxia telangiectasia mutated (ATM) gene cause the disease, so we wanted to explore the differences in various parts of the DNA damage response pathway, such as γ H2A.X, 53BP1, R-loops, and ATM, between healthy cells and AT patient-derived cells, more specifically in neural progenitor cells from age-matched healthy controls and AT patients. To investigate the differences, ionizing radiation was done to induce DNA damage in both the control and AT cell lines and given different recovery time points, which was followed by immunofluorescence staining on γ H2A.X and 53BP1, as well as western blots to quantify the levels of γ H2A.X. We discovered that the increase in γ H2A.X levels were not as significant in AT cells when compared to the controls. Additionally, dot blots were used to assess global R-loop changes in AT cells, in which R-loop accumulation was higher in AT cells, with a further increase in R-loop accumulation after IR treatment. qPCR sequencing was done to compare ATM mRNA expression, and we discovered that there were lower levels of ATM mRNA expression in AT cells. From the data, we can conclude that AT is potentially caused by dysregulation of the DDR pathway, specifically through impairment or less transcription of ATM.

Introduction

Ataxia Telangiectasia (AT) is an autosomal recessive neurodegenerative disease, and it is an early childhood onset disease that affects 1 in 40,000 to 100,000 people (Rothblum-Oviatt et al., 2016). AT affects the part of the brain that controls motor movement, causing difficulty coordinating movement, immune defects, and radiosensitivity or the susceptibility of various neuronal cell types to the harmful effect of ionizing radiation (Arnould et al. 2023). The disease is caused by various mutations in the ataxia telangiectasia mutated (ATM) gene (Paull 2015). Some mutations may be frameshift or nonstop, missense, or in-frame deletions, with majority creating an irregular stop codon in the sequence to lead to a loss-of-function in ATM (Karlsson et al., 2021). The mutated gene leads to protein instability, decreased functional protein, or reduced kinase activity. The ATM protein plays a critical role in multiple cell-signaling cascades as a kinase, of significance being the DNA damage response (DDR) pathway (McKinnon, 2004). ATM is activated by double-strand breaks (DSBs) to phosphorylate many substrates and activate signaling pathways for DDR. ATM loss-of-function in AT can impair DDR and alter gene expression.

γ H2A.X is produced when the histone variant H2A.X is phosphorylated on the Ser-139 residue in response to DNA DSBs (Mah et al., 2010). Inhibition of ATM abolishes γ H2A.X-domain formation, which comprises DSB clustering. γ H2A.X is a molecular marker of DNA damage and repair as well as an early cellular response to the induction of DNA double-strand breaks. γ H2A.X decorates chromatin in the D compartment, a new chromatin compartment where its formation is driven by ATM, acts to signal DDR, and γ H2A.X decorates the chromatin after DSB induction (Arnould et al. 2023). The production of γ H2A.X increases with increasing

DNA damage, but ATM is specifically responsible for ionizing radiation (IR)-induced production of γ H2A.X (Friesner et al., 2005).

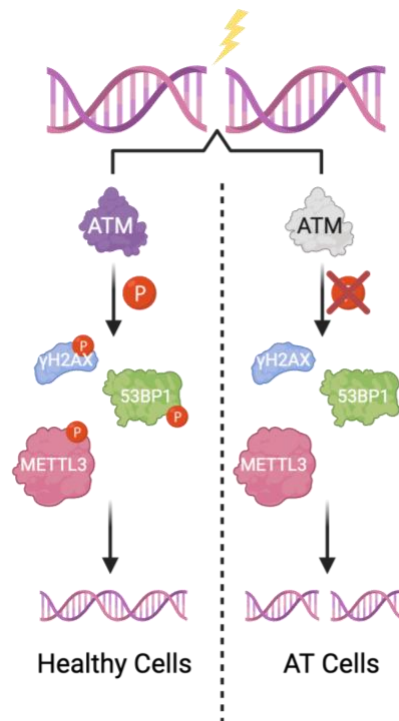
The tumor-suppressor protein p53 Binding Protein 1 (53BP1) gets phosphorylated by ATM at multiple sites. 53BP1 has a role in DDR as it localizes to DNA DSBs when cells are exposed to IR. The protein is also accompanied by the presence of γ H2AX, which is another marker of DNA damage. The amount of 53BP1 increases over time after irradiation, and closely parallels the number of DNA DSBs (Mochan et al., 2004). 53BP1 likely binds to long stretches of DNA or chromatin on either side of the DNA DSBs (Mochan et al., 2004).

A potential mechanism for AT pathogenesis is the R-loop dysregulation within motor neurons. R-loops are three-stranded DNA-RNA structures composed of a DNA-RNA hybrid and a non-template DNA strand (Crossley, Bocek, and Cimprich 2019). They have emerged as key components of DSB-mediated DDR. R-loops have critical roles in both causing and responding to DSBs, which would implicate their role in numerous diseases (Marnef and Legube 2021). The presence of R-loops near DSBs recruits cellular machinery to repair the initial damage. DDR-upregulated genes targeted to the D compartment displayed high levels of R-loops compared to genes that were not targeted to the D compartment (Arnould et al. 2023). Impairment of R-loops processing may lead to an accumulation of DSBs (Allison and Wang 2019), contributing to the progression of neurodegenerative diseases such as AT.

Methyltransferase-like 3 (METTL3) protein, an RNA N6-methyl adenosine (m6A) methyltransferase is identified as a substrate of the ATM kinase. The m6A on the RNA strand of R-loops affects R-loop formation during DSB repair. ATM phosphorylates METTL3 in response to DSBs. The relationship between ATM-METTL3 phosphorylation in response to DNA damage and regulation of R-loop formation through m6A deposition could play crucial roles in AT

pathogenesis but has yet to be defined. Ribonuclease (RNase) H enzymes, or more specifically RNase H1, degrade the R-loop RNA chains by binding to the m6A-modified R-loops to catalyze resolution (Zhang et al., 2024). AT-rich interactive domain 1A (ARID1A), a member of the SWI/SNF family, regulates gene transcription by altering chromatin structure, but it also facilitates the recruitment of METTL3 to DSBs. ARID1A acts in an ATM-dependent manner in its recruitment to R-loops (Zhang et al., 2024).

As we can see, many components of the DDR pathway are regulated by ATM (Supplementary Figure 1), so we wanted to explore how healthy and AT patient-derived cells differ in the expression of all these different components. We look into the differences between healthy and AT cells in γ H2A.X, 53BP1, ATM, and R-loop accumulation, predicting higher levels of γ H2A.X and 53BP1 and lower levels of ATM, and R-loop accumulation.

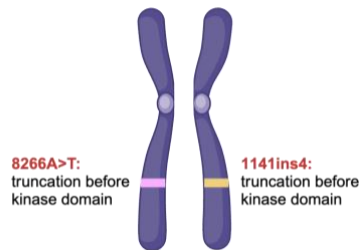


Supplementary Figure 1. ATM as a master regulator of the DNA damage response pathway. Figure made by Katherine Westover on BioRender.

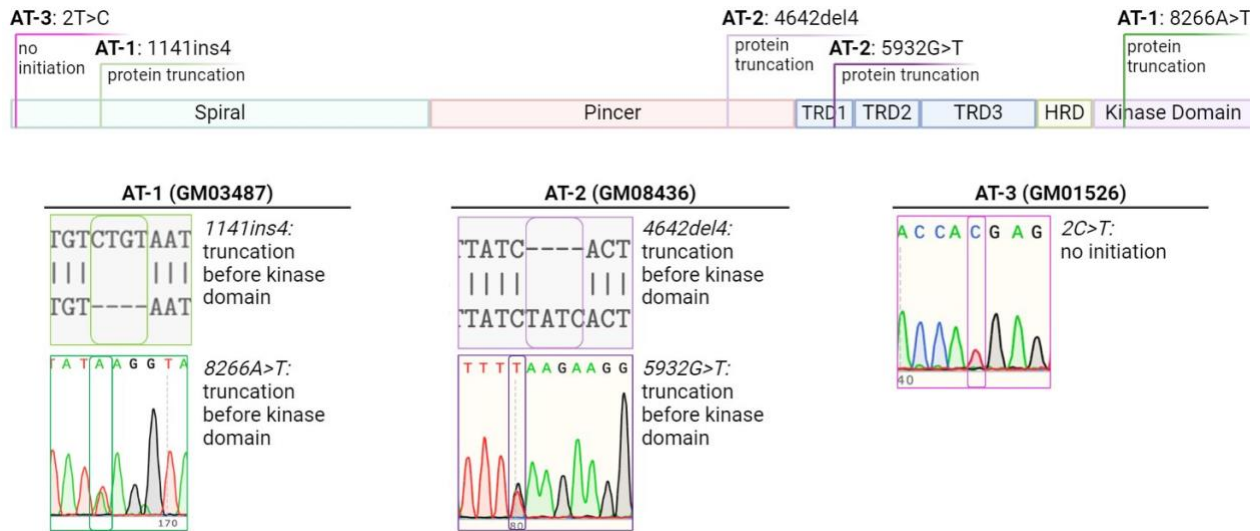
Materials and Methods

Cell-Line Information

Lymphoblastoid cell lines (LCLs) and fibroblasts were obtained from the Coriell Biobank for the AT patient cell lines and one of the healthy control cell lines. The AT cell lines that were obtained are as follows: GM03487 (AT-1), GM08436 (AT-2), GM01526 (AT-3). The healthy controls that were used in this project were 426 (C-2) and 427 (C-3). The cell line 427 (C-3) was received from the Zhexing Wen lab at Emory University. AT-1 is a compound heterozygote with the mutations 1141ins4 and 8266A>T; both mutations cause a truncation before the kinase domain (Supplementary Figure 2). AT-2 is also a compound heterozygote, but with the mutations 4642del4 and 5932G>T, both causing truncations before the kinase domain. AT-3 is a homozygote with the mutation 2C>T that causes no initiation of translation of the gene (Supplementary Figure 3). The healthy controls are somewhat age-matched to the AT lines.



Supplementary Figure 2. AT-1 is a compound heterozygote with the mutation 1141ins4 on one allele and the mutation 8266A>T on the other allele. Both mutations cause a truncation before the kinase domain. Figure made on BioRender.



Supplementary Figure 3. Schematic showing all the mutations on *ATM* and the outcome of each mutation. Figure made by Katherine Westover on BioRender.

Reprogramming LCLs and Fibroblasts

LCLs and Fibroblasts were reprogrammed into induced pluripotent stem cells (iPSCs) with the introduction of Yamanaka factors (Oct4, Sox2, Klf4, and c-Myc) by viral gene transfer. The iPSCs were then differentiated into neural progenitor cells (NPCs) using differentiating media

Ionizing Radiation (IR)

Both healthy and control cell lines were exposed to IR at 10 Gray, which induces DNA damage or double-stranded breaks. The cells were given 6 hours to respond to the damage, which is an acute response, and then collect gDNA, RNA, and protein to see how the cells respond molecularly to damage.

RT-qPCR

A Template Mix with 1 μ L of the template cDNA, 1 μ L of 5 μ M Forward and Reverse primer, 10 μ L of SYBR Green Mix (QuantaBio #95074), and 8 μ L of Nuclease-free water was prepared. If

there are different primers used for different samples, both the cDNA and primers should be excluded from the Template Mix. It was pipetted up and down to mix thoroughly followed by a vortex and a brief spin. Load the 96-well plate (Thermo #4483354) with 19 μ L of the Template Mix and 1 μ L of the cDNA/primers that were excluded with Rainin tips and completely release the liquid in the well. An adhesive cover (Thermo #4360954) was placed over the plate. The plate was then vortexed to mix and placed on ice. The plate was spun down using a plate spinner. It was then run by the QuantStudio 3 RT-PCR System, with the reaction settings in the order of 95°C for 10 minutes, 95°C for 15 seconds, 60°C for 1 minute, and repeated for 40 cycles.

Immunofluorescence Staining

The media was aspirated from the wells. The cells were washed with 1 mL of 1X PBS for 5 minutes and aspirated off; the wash step was repeated three times. The cells were then washed with 600 μ L of 4% PFM for 20 minutes and aspirated off. The cells were washed with 1 mL of 1X PBS for 5 minutes and aspirated off; the wash was repeated three times. The cells were washed with 600 μ L of 0.5% Triton X-100 for 15 minutes and aspirated off. The cells were washed with 1 mL of 1X PBS for 5 minutes and aspirated off; the wash was repeated three times. The cells were washed with 600 μ L of 5% NGS (added drop-wise to ensure the entire coverslip is covered) for 30 minutes. The primary antibody, Rabbit hSUN1, was added in a 1:400 dilution. It was incubated at 4°C overnight in the dark. For the following, all was done in the dark. The primary antibody was collected to re-use and stored at -20°C. The cells were washed with 1 mL of 1X PBS for 5 minutes and aspirated off; the wash step was repeated 3 times. The primary antibody was added at an appropriate dilution in 5% NGS. It was incubated at room temperature for 2-3 hours in the dark. The cells were washed in 1 mL of 1X PBS for 5 minutes and aspirated off; the wash step was repeated three times. The slides were prepared by adding approximately

20 μ L of Slow Fade Gold antifade DAPI to the slide and the cover slip was placed cell-side down over the DAPI. It was dried for 24 hours at 4°C in the dark.

Western Blot

The protein samples were heated in a 98°C heatblock for 10 minutes. The gel to run the western blot was set up. Running buffer was prepared by mixing 540 mL of milliQ water and 60 mL of buffer. A precast gel was removed from the packaging and placed in the western blot apparatus ensuring no leaks from the center of the apparatus. The running buffer was added to the middle of the apparatus until full and the rest of the buffer was added to the tank, ensuring that the metal wire was covered by the buffer. The well comb was removed. A protein ladder and the samples were added to the gel. It was run at 80V for 15-20 minutes to ensure the ladder was separating on the gel. It was then run at 120V until done. The gel was removed from the casing without drying the gel and transferred to the transfer pack. The gel was lined up with the transfer membrane and the top of the transfer pack was placed. It was rolled to remove any bubbles. A transfer machine was used to transfer using the TGX mini protocol. Once the transfer was complete, the membrane was moved to a new container and blocked with 5% milk for 1 hour. The membrane was cut as needed. A primary antibody, γ H2A.X and α -Tubulin, was added with an appropriate dilution (1:5000) and left to incubate on a tilting platform at 4°C overnight. The membrane was quickly washed three times with 0.05% TBST. The membrane was washed three 5-minute washes with 0.05% TBST on the rt-shaker. The membrane was incubated with the secondary antibody, anti-rabbit for γ H2A.X and anti-mouse for α -Tubulin, in a 1:5000 dilution in 5 % milk on the rt-shaker for 1-2 hours. The membrane was quickly washed three times with 0.05% TBST. The membrane was washed three 5-minute washes with 0.05% TBST on the rt-shaker. The blot was imaged after developing with ECL.

gDNA Isolation

The cells were cultured to 75-80% confluency in a 10-cm dish. The culture medium was aspirated and then washed with 37°C pre-warmed 1X DPBS. The DPBS was aspirated and 1.5 mL of 0.05% (wt/vol), 1X trypsin-EDTA at 37°C was added. It was left for 2 minutes to dissociate the cells from the dish. 5 mL of 37°C complete medium was added to stop the reaction and pipetted. The contents were transferred to a 15-mL tube and was spun at 800 G for 3 minutes to pellet the cells. The cells were washed by resuspending them in 5 mL of 1X DPBS. The cells were spun gently at 1,000 RPM for 3 minutes to pellet the cells. The cells were resuspended in 1.6 mL of TE buffer. 50 µL of 20% (wt/vol) SDS and 5 µL of 20 mg/mL proteinase K were added. The tubes were inverted gently five to six times until the solution became viscous. The tubes were incubated at 37°C overnight (12-14 hours). 15-mL high-density Maxtract phase-lock gel tubes were spun for 1 minute at 1500 G to pellet the gel. The DNA lysate was poured into the phase-lock gel tube and 1 volume (1.6 mL) of phenol/chloroform/isoamyl alcohol (25:24:1) was added. The tubes were inverted four to five times gently and spun down at 1500 G for 5 minutes. 1/10 volume (160 µL) of 3 M NaOAc, pH 5.2 and 2.5 volumes (4 mL) of 100% (vol/vol) ethanol was added to a new 15-mL tube. The DNA (top aqueous phase) from the phase-lock gel tube was poured into the tube and mixed by gently inverting the tube until the DNA fully precipitates. The DNA was spooled out of the mixture with cut tips and transferred to a clean 2-mL tube. The DNA was washed by adding 1.5 mL of 80% (vol/vol) ethanol, gently inverting the tube two to three times and letting it sit for 10 minutes. The supernatant was discarded without disturbing the DNA; the wash step was repeated two more times. After the last wash, as much ethanol as possible was removed by pipetting. The DNA was left to air-dry completely while inverting the tube and 125 µL of TE buffer was added directly to the DNA pellet. It was then kept on ice for

an hour. The DNA was gently resuspended by pipetting two to three times with a 200- μ L cut tip. It was left on ice for at least another before the restriction enzyme digest. 50-100 μ L of extracted genomic DNA was digested using a cocktail of restriction enzymes (50-100 μ L of DNA, 15 μ L of NEBbuffer 2, 1.5 μ L of BSA, 30 μ L of each restriction enzyme, up to 150 μ L of water, and 1.5 μ L of 0.5X spermidine). The digestion was incubated overnight at 37°C. 2-mL 'phase-lock gel, light' tubes were spun for 1 minute at 16,000 G to pellet the gel. The DNA was gently pipetted from the previous step into the phase-lock gel tube. 100 μ L of water and 1 volume (250 μ L) of phenol/chloroform/isoamyl alcohol (25:24:1) were added. The tubes were gently inverted four to six times then spun down at 16,000 G for 10 minutes. In a clean 1.5-mL tube, 1.5 μ L of glycogen, 1/10 volume (25 μ L) of 3 M NaOAc, pH 5.2, and 2.5 volumes (625 μ L) of 100% (vol/vol) ethanol were added. The DNA was gently pipetted from the phase-lock gel tubes and mixed by inverting four to six times. It was incubated for at least an hour at -20°C. It was spun at 16,000 G for 35 minutes at 4°C. The supernatant was discarded and 200 μ L of room-temperature 80% (vol/vol) ethanol was added. It was spun for 10 minutes at 16,000 G at 4°C and the supernatant was discarded. The pellet was air-dried for 15-25 minutes depending on the DNA concentration and resuspended in 50 μ L of TE buffer. The tubes were left on ice for 30-60 minutes and then gently resuspended.

Dot Blot

A dilution of each sample was prepared so that there was 100 μ g/ μ L of DNA. Those dilutions were then used to make dilutions in PCR tube strips so that there was 1 μ g and 0.5 μ g of DNA for each sample. The dot-blot apparatus was prepared, and the membrane was pre-wet with 6X SSC for 1-2 minutes. The membrane was placed on the Bio-Pad and the rest of the Bio-Pad was covered with plastic wrap. The lid was placed and screwed on tightly. The dot-blot was attached

to a vacuum and the vacuum was turned on. To confirm it was working, removal of any wetness from the membrane within the wells was observed. 40 μ L of the samples were loaded using a single-channel pipette without touching the membrane. The wells were then washed with 200 μ L of 6X SSC two times. The vacuum was left to run at room temperature for 15 minutes. With the vacuum still on, the lid was unscrewed and removed to carefully peel off the membrane using forceps and placed on a clean KimWipe. It was placed in an 85°C incubator for 30 minutes. The membrane was then incubated in 5% non-fat milk on the shaker for 30 minutes at room temperature. An appropriate amount of primary antibody, S9.6, is added in a 1:5000 dilution to the blocking solution. It was incubated at 4°C overnight on the tilting platform. The membrane was washed in 0.05% TBST briefly three times, then washed again 3 times for five minutes each at 70 RPM on the shaker. The secondary antibody, IgG anti-mouse, was added in a 1:5000 dilution to the blocking solution and incubated at room temperature for 1 hour at 50 RPM. The membrane was washed in 0.05% TBST briefly three times, then washed again 3 times for five minutes each at 70 RPM on the shaker. The membrane was imaged after developing with ECL.

Results

AT Cells Present Lower Expression of ATM mRNA

qPCR-sequencing was done to determine the differences in ATM mRNA expression between healthy and AT cells and validate the loss-of-function of ATM. The qPCR results show that AT patient-derived cell lines had lower mRNA expression levels for both primers ATM1 and ATM2 when compared to healthy cells (Figure 1). From this, we can infer that there are lower levels of mRNA, which could further suggest lower ATM protein levels.

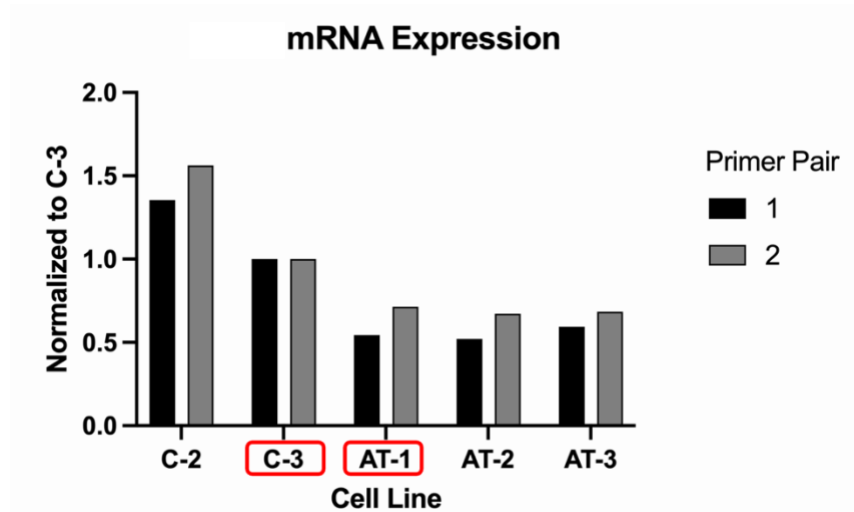


Figure 1. qPCR results showing mRNA expression for the cell lines AT-1 (03487), AT-2 (08436), AT-3 (01526), C-2 (426), and C-3 (427). The bar graph was normalized to C-3 to illustrate the comparative mRNA expression of the various cell lines.

Differences in γ H2A.X and 53BP1 Levels Between Healthy and AT Cells

γ H2A.X is known to be a molecular marker for DNA damage and repair, so immunofluorescence staining was done to investigate whether there was a difference in the γ H2A.X levels between the healthy and AT cell lines. We observed an increase in γ H2A.X loci in healthy cells (Figure 2). There was also an increase in 53BP1 loci in healthy cells (Figure 3), further showing that there was DNA damage induced after IR treatment. To further support this, our western blots have shown similar results. The γ H2A.X levels are significantly greater after IR treatment in healthy cells (Figure 4A & B). This suggests that the IR treatment worked in inducing DNA damage. In the AT cells, there was still an increase in the γ H2A.X levels, or the phosphorylation of H2A.X, but not as much as the controls, suggesting an impaired function of ATM in the DDR pathway (Figure 4A & B). From these results, we can infer AT causes an impaired function of ATM, affecting γ H2A.X levels in the DDR pathway.

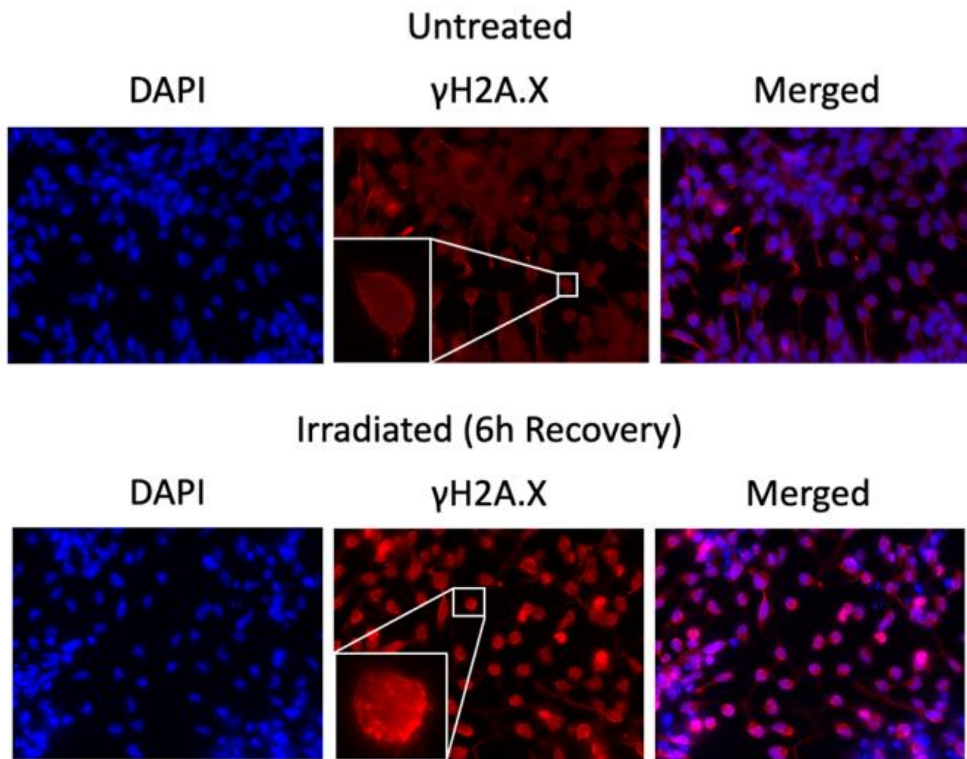


Figure 2. Immunofluorescence staining 427(C) cells before and after IR treatment for γ H2A.X.
 (A) Immunofluorescence staining of control cell line before IR treatment for γ H2A.X. (B) Immunofluorescence staining of control cell line after IR treatment for γ H2A.X.

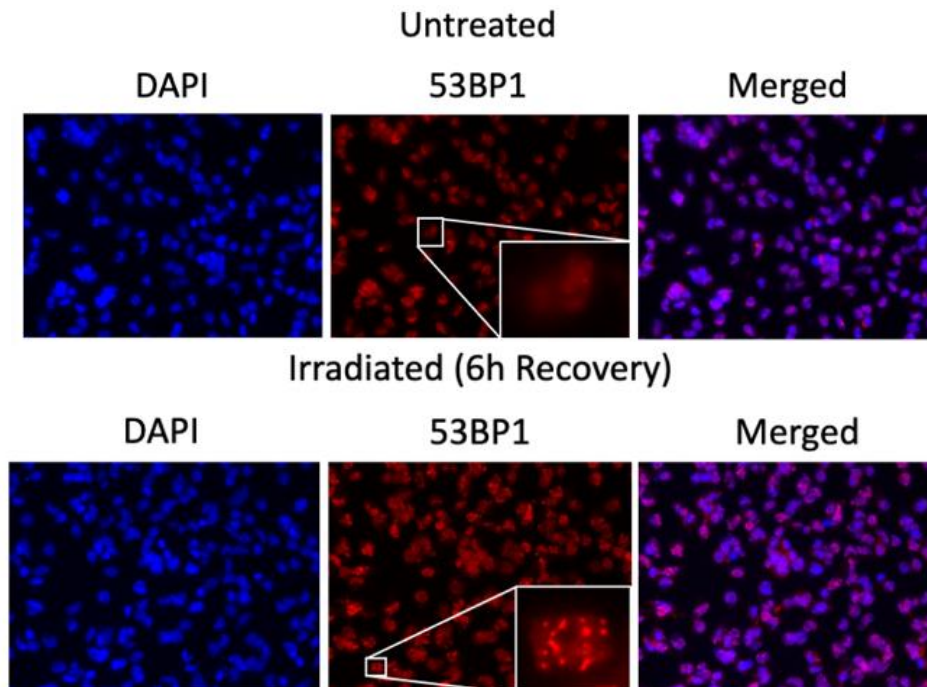


Figure 3. Immunofluorescence staining of 53BP1 for 427 (C) before and after IR treatment.
 Immunofluorescence staining of 53BP1 for the healthy control cell line before and after IR treatment.

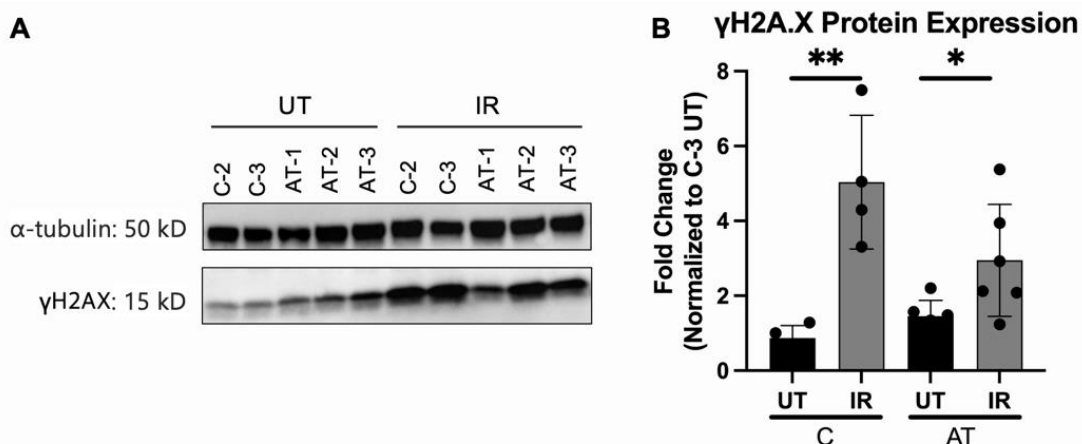


Figure 4. Western blots and quantifications of γ H2A.X and H2A.X in control and AT cell lines before and after IR treatment. (A) Western blot of control and AT cell lines before, or untreated (UT), and after IR treatment. (B) Bar graph depicting the γ H2A.X levels in control and AT cell lines by quantifying two western blots, showing the significance of the increase γ H2A.X after IR treatment in control cells.

R-loop Accumulation in AT

Dot blots were done to investigate the differences in R-loop accumulation between AT and healthy cells. To demonstrate that the dot blots were presenting R-loops, RNase H treated AT, and healthy cells were used as a negative control, as RNase H resolves R-loops. S9.6 was used as the primary antibody, a mouse monoclonal antibody that recognizes DNA-RNA hybrids. AT cell lines have a higher accumulation of R-loops before IR treatment (Figure 5A & B), suggesting the AT cells have an impaired DDR response. After IR treatment, there is also an increased accumulation of R-loops as recovery time for the cells after IR treatment increases (Figure 6A & B). The impairment of R-loop processing in AT cells can explain an accumulation of DSBs, which can further demonstrate the effect R-loops have on the progression of AT.

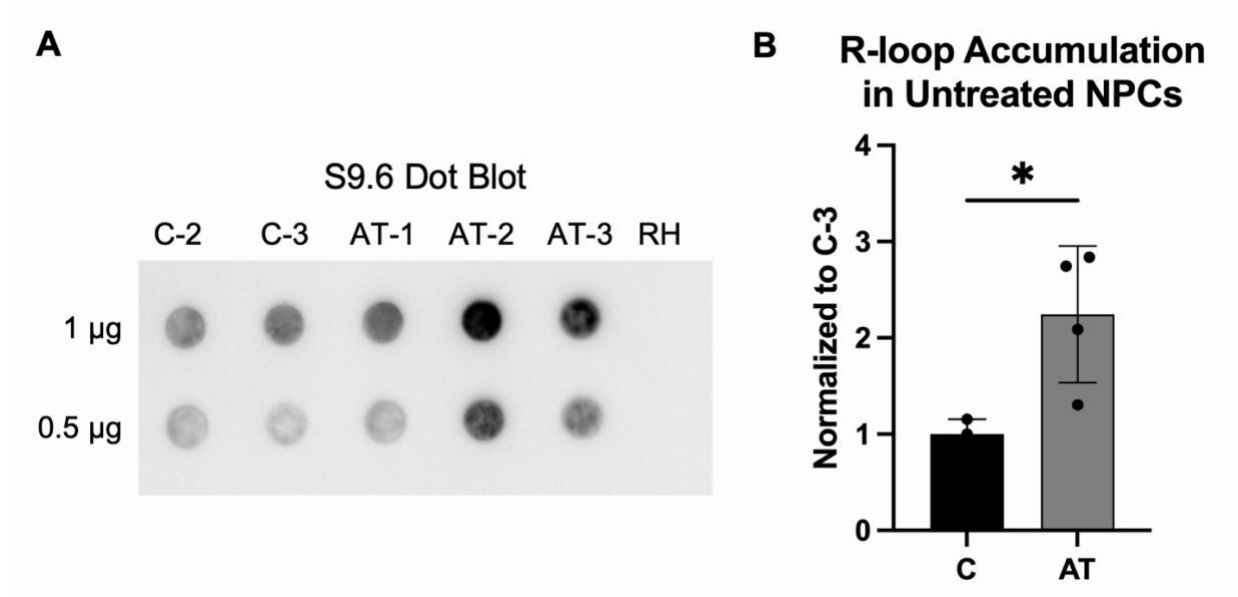


Figure 5. Dot blot and graph with various C and AT cell lines before IR treatment. (A) Dot blot showing R-loop accumulation for C-2 (426), C-3 (427), AT-1 (03487), AT-2 (08436), and AT-3 (01526) with samples containing 1 µg and 0.5 µg of DNA before IR treatment. (B) Bar graph showing a higher abundance of R-loops in AT cells based on the quantified intensity of the dots in various dot blots. The bar graph was normalized to the control untreated samples.

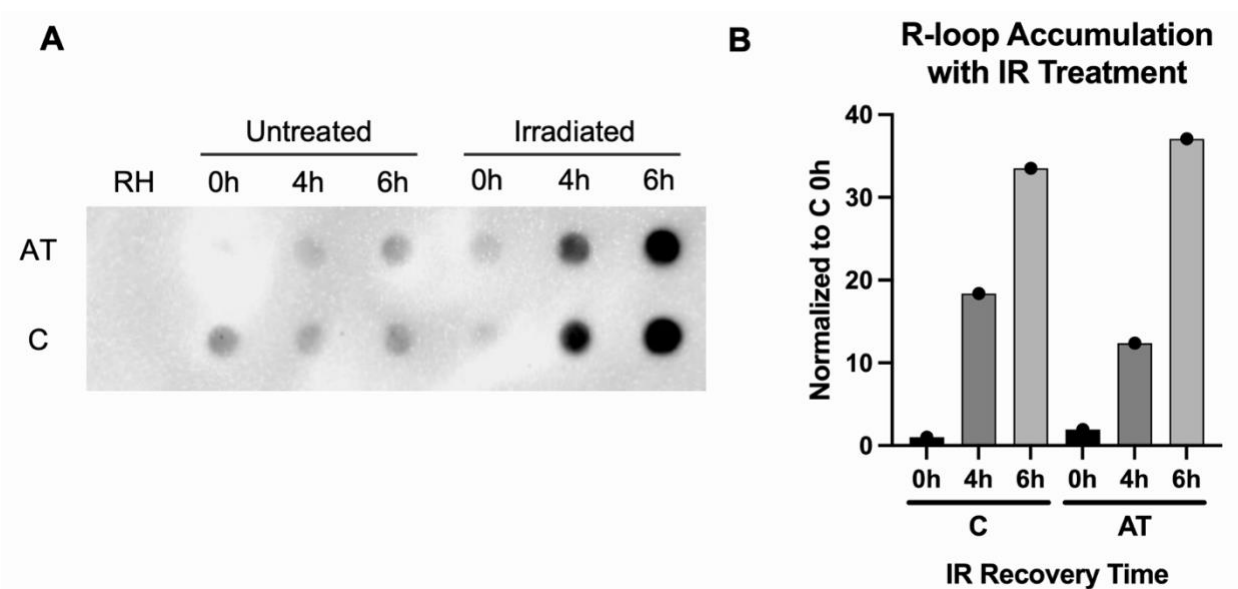


Figure 6. Dot blot for C (426) and AT (08436) cell lines before and after IR treatment at various time points to show the accumulation of R-loops over time after DNA damage was induced. (A) Dot blot for C and AT cell lines to illustrate there was an increase in global R-loop accumulation after DNA damage was induced at 0h, 4h, and 6h. (B) Bar graph to show the increase in global R-loop levels after IR treatment with various recovery times. Only one blot was quantified for this graph, so no statistical analysis was done. Note that the scale is different from Figure 5B.

Discussion

The differences between healthy and AT cells are still yet to be fully understood. However, from our studies, we can see that AT is potentially caused by dysregulation of the DDR pathway, more specifically, through ATM loss of function or decreased levels of ATM, which lead to an accumulation of R-loops in AT cells. We further studied how AT cells respond to induced DNA damage by irradiating the cells with ionizing radiation and found that much of the data supports the hypothesis that ATM is a crucial component in the DDR pathway, and the lack of ATM has an effect on AT cells.

AT Cells Present Differences in ATM Transcription Levels

To understand if ATM is one of the crucial factors in causing the impairment in the DDR pathway, qPCR was done to check the ATM mRNA expression levels, which would allow us to see the difference in ATM transcription levels between healthy and AT cells. The nature of mutations in AT patients is loss-of-function of ATM. We found that AT cells have lower levels of ATM mRNA expression for both primers ATM1 and ATM2. This would explain the impairment of the DDR pathway mentioned in earlier sections. Many processes involved in the DDR pathway are ATM-dependent, such as the phosphorylation of H2A.X to form γ H2A.X, the phosphorylation of 53BP1, and the resolution of R-loops.

Differences in γ H2A.X and 53BP1 Levels Between Healthy and AT Cells

To understand the differences between healthy and AT cells in terms of γ H2A.X and 53BP1, we examined the levels of each DNA damage biomarker. For both biomarkers, immunofluorescence staining was done to illustrate the DNA damage present before and after IR

treatment. For both γ H2A.X and 53BP1, we found that there was an increase in γ H2A.X and 53BP1 levels in the healthy cells after IR treatment, proving the IR treatment worked in inducing DNA damage. There was also little to no change in the H2A.X levels, which shows that the increase in γ H2A.X in healthy cells is due to increased phosphorylation of H2A.X. This also explains the lower increase in γ H2A.X in AT cells is due to low phosphorylation of H2A.X, possibly due to low ATM levels or impaired function of ATM. The AT cells have higher γ H2A.X levels when compared to healthy cells before IR treatment, possibly due to higher levels of DNA damage. The lower increase after IR treatment in AT cells, would be explained by dysregulation of the DDR pathway. We still see an increase after inducing damage, however, because γ H2A.X phosphorylation is done not only by ATM but also other types of enzymes like ATR.

R-loop Accumulation in AT

R-loops have been studied in the context of the DDR pathway, and they play a role in leading to DSBs. Our findings show that there is a significantly higher abundance of R-loops in AT cells even before IR treatment when compared to healthy cells, which suggests an impaired DDR response in the AT cells. For the dot blots, RNase H treatments were done on healthy and AT cells to show that the dot blots indeed show R-loop abundance. RNase H may resolve R-loops in-vivo after binding to m⁶A modifications, which are created by METTL3. METTL3 is recruited to DSBs with the help of ARID1A, which is ATM-dependent for recognizing R-loops. We also observed an increase in R-loops as IR recovery time increases. With lower ATM levels or impaired function of ATM, ARID1A would not be able to recognize R-loops to help METTL3 get recruited to DSBs, and lower the resolution of R-loops by RNase H. The accumulation of R-

loops with increased IR recovery times can be explained by an impaired DDR response in AT cells due to less ATM. The accumulation of R-loops may be an underlying factor in AT progression.

Some limitations of this research would be that there are no western blots with quantifications to back up both the 53BP1 and ATM results. With the western blot attempts for 53BP1 and ATM, the blots were inconclusive. Future studies would include western blots for both 53BP1 and ATM to confirm protein levels of both and dysregulation of the DDR pathway. IF staining could also be done for ATM to further confirm its presence in AT cells. RNA-sequencing and DRIP-sequencing would also be done to identify the loci-specific R-loop changes and correlate that with the gene expression. Future studies could also be done to study the effects that the phosphorylation of METTL3 would have on R-loop accumulation, such as checking phosphorylation levels of METTL3 after knockout of ATM, and how that may underlie AT progression.

From our data, we can conclude that AT is potentially caused by dysregulation of the DDR pathway, specifically through impairment ATM or less transcription of ATM, which shows a smaller increase of γ H2A.X levels and a greater accumulation of R-loops that could underlie the progression of AT.

References

- Allison, D. F., & Wang, G. G. (2019). R-loops: Formation, function, and relevance to cell stress. *Cell Stress*, 3(2), 38–46. <https://doi.org/10.15698/cst2019.02.175>
- Arnould, C., Rocher, V., Saur, F., Bader, A. S., Muzzopappa, F., Collins, S., Lesage, E., Le Bozec, B., Puget, N., Clouaire, T., Mangeat, T., Mourad, R., Ahituv, N., Noordermeer, D., Erdel, F., Bushell, M., Marnef, A., & Legube, G. (2023). Chromatin compartmentalization regulates the response to DNA damage. *Nature*. <https://doi.org/10.1038/s41586-023-06635-y>
- Crossley, M. P., Bocek, M., & Cimprich, K. A. (2019). R-Loops as Cellular Regulators and Genomic Threats. *Molecular Cell*, 73(3), 398–411. <https://doi.org/10.1016/j.molcel.2019.01.024>
- Friesner, J. D., Liu, B., Culligan, K., & Britt, A. B. (2005). Ionizing Radiation– dependent γ -H2AX Focus Formation Requires Ataxia Telangiectasia Mutated and Ataxia Telangiectasia Mutated and Rad3-related. *Molecular Biology of the Cell*, 16.
- Karlsson, Q., Brook, M. N., Dadaev, T., Wakerell, S., Saunders, E. J., Muir, K., Neal, D. E., Giles, G. G., MacInnis, R. J., Thibodeau, S. N., McDonnell, S. K., Cannon-Albright, L., Teixeira, M. R., Paulo, P., Cardoso, M., Huff, C., Li, D., Yao, Y., Scheet, P., ... Kote-Jarai, Z. (2021). Rare Germline Variants in ATM Predispose to Prostate Cancer: A PRACTICAL Consortium Study. *European Urology Oncology*, 4(4), 570–579. <https://doi.org/10.1016/j.euo.2020.12.001>
- Mah, L.-J., El-Osta, A., & Karagiannis, T. C. (2010). γ H2AX: A sensitive molecular marker of DNA damage and repair. *Leukemia*, 24(4), 679–686. <https://doi.org/10.1038/leu.2010.6>
- Marnef, A., & Legube, G. (2021). R-loops as Janus-faced modulators of DNA repair. *Nature Cell Biology*, 23(4), 305–313. <https://doi.org/10.1038/s41556-021-00663-4>
- McKinnon, P. J. (2004). ATM and ataxia telangiectasia. *EMBO Reports*, 5(8), 772–776. <https://doi.org/10.1038/sj.embor.7400210>
- Mochan, T. A., Venere, M., DiTullio, R. A., & Halazonetis, T. D. (2004). 53BP1, an activator of ATM in response to DNA damage. *DNA Repair*, 3(8–9), 945–952. <https://doi.org/10.1016/j.dnarep.2004.03.017>
- Paull, T. T. (2015). Mechanisms of ATM Activation. *Annual Review of Biochemistry*, 84(1), 711–738. <https://doi.org/10.1146/annurev-biochem-060614-034335>

Rothblum-Oviatt, C., Wright, J., Lefton-Greif, M. A., McGrath-Morrow, S. A., Crawford, T. O., & Lederman, H. M. (2016). Ataxia telangiectasia: A review. *Orphanet Journal of Rare Diseases*, 11(1), 159. <https://doi.org/10.1186/s13023-016-0543-7>

Zhang, J., Chen, F., Tang, M., Xu, W., Tian, Y., Liu, Z., Shu, Y., Yang, H., Zhu, Q., Lu, X., Peng, B., Liu, X., Xu, X., Gullerova, M., & Zhu, W.-G. (2024). The ARID1A-METTTL3-m6A axis ensures effective RNase H1-mediated resolution of R-loops and genome stability. *Cell Reports*, 43(2), 113779. <https://doi.org/10.1016/j.celrep.2024.113779>